Fermi National Accelerator Laboratory

FERMILAB-Conf-93/362-E

CDF

b Production at CDF

Daniel A. Crane
For the CDF Collaboration

Fermi National Accelerator Laboratory
P.O. Box 500, Batavia, Illinois 60510

January 1994

Presented at the *9th Topical Workshop on Proton-Antiproton Collider Physics*,
Tsukuba, Japan, October 18-22, 1993

Disclaimer

CDF/PUB/BOTTOM/PUBLIC/2352
FERMILAB-CONF-93/362-E

b Production at CDF

Daniel A. Crane*
Fermilab
Batavia, Illinois 60510, USA
For the CDF Collaboration

Abstract

The production of b quarks in $p\bar{p}$ collisions is studied in the Collider Detector at Fermilab (CDF), using the B meson decay channels $B^+ \to J/\psi K^+$ and $B^0 \to J/\psi K^{*0}$, with $J/\psi \to \mu^+\mu^-$ and $K^{*0} \to K^+\pi^-$, and their charge conjugates. Measurements of the B meson and b quark cross-sections integrated above minimum transverse momentum values in the rapidity range $|y| < 1$ are described. The first fully differential B meson cross-section measurement, in the same rapidity range, is also reported. Comparison is made to the $O(\alpha_s{}^3)$ theoretical calculations.

The study of heavy flavor production at the highest center-of-mass energy currently available provides the opportunity to check the accuracy of the perturbative expansion of the cross-section in terms of α_s, the QCD coupling constant. There exist QCD calculations at next-to-leading order ($\mathcal{O}(\alpha_s{}^3)$) [1, 2] which, along with recent preliminary parameterizations of the parton distribution functions down to $x \approx 10^{-5}$ [3], predict the b quark cross-section. It is necessary to show that these predictions provide an adequate description of the cross-section at 1.8 TeV before they can be confidently extrapolated to higher energies or more exotic phenomena.

The B meson and b quark cross-sections in $p\bar{p}$ collisions at $\sqrt{s} = 1.8$ TeV are measured using the exclusive decay channels $B^+ \to J/\psi K^+$ and $B^0 \to J/\psi K^{*0}$, with $J/\psi \to \mu^+\mu^-$ and $K^{*0} \to K^+\pi^-$, and their charge conjugates. The J/ψ is required to decay to two muons, a mode which is easily detected at the trigger level. The dimuon triggers have proven in the past to provide a reliable sample of J/ψ, and it has recently been shown that in the transverse momentum range of interest, more than 15% of the sample comes from B decays [4]. The data sample represents $(14.3 \pm 1.0) pb^{-1}$ collected by the Collider Detector at Fermilab (CDF) during the 1992-93 run. CDF has measured the integrated cross-sections using these decay channels before [5, 6], but increased statistics now also allows measurement of the differential cross-section as a function of the transverse momentum, p_T.

*Presented at the 9th Topical Workshop on Proton - Antiproton Collider Physics, Tsukuba, Japan, October 18-22, 1993.

Detailed descriptions of the CDF detector have been provided elsewhere [7]. Here a brief description of the components used in this analysis is presented. The z-axis of the detector coordinate system is along the beam direction. The Central Tracking Chamber (CTC) is a drift chamber, consisting of nine superlayers; five give information on the track in the $R-\phi$ transverse plane, and the other four give z information. To be able to pass through all nine superlayers, a particle must have pseudorapidity $|\eta| < 1$, where $\eta \equiv -\ln(\tan(\theta/2))$. This geometrical requirement dictates the rapidity range for the cross-section calculation. An axial magnetic field of 1.4 T is present throughout the CTC volume.

Surrounding the CTC are electromagnetic and hadronic calorimeters, which contain approximately five absorption lengths of material for pions at normal incidence. Outside the calorimeters are the central muon chambers, segmented into 72 modules providing about 85% coverage in ϕ in the pseudorapidity range $|\eta| < 0.6$. Each module consists of four layers of wire chambers equally spaced in R. Muon candidate tracks are formed when at least three of the four sense wires register a hit.

The selection of B candidates begins by identifying J/ψ candidates that decay to two muons. There are three levels of trigger requirements that must be passed for a muon pair to be included in the J/ψ data sample. At the first trigger level, two muon candidates must have been detected in the central muon chambers. A cut is made on the slope of the track in the $R-\phi$ plane which corresponds to a cut in transverse momentum. The efficiency for this trigger rises from 50% at $p_T = 1.8$ GeV/c to 90% at $p_T = 3.8$ GeV/c. The muon chamber tracks must be separated by at least 0.09 radians in ϕ. The second trigger level requires at least one of the muons to match a track found in the CTC by a fast hardware track processer. The efficiency for the track processer rises from 50% at 2.7 GeV/c to 90% at 3.4 GeV/c. At the third trigger level CTC pattern recognition and tracking are done. Cuts are made on the probability of the match between a CTC track and the muon chamber track. The dimuon invariant mass is required to be within a 600 MeV/c^2 window about the world-average J/ψ mass. The minimum transverse momentum allowed for either muon is 1.4 GeV/c, since prompt muons with lower momentum are unlikely to reach the muon chambers due to energy loss from ionization.

After offline reconstruction is performed, additional cuts are imposed to further improve the purity of the J/ψ sample. Higher probability of a match between the CTC track and the muon chamber track is required. Transverse momentum cuts motivated by the data are applied to the muons at the points where the rising trigger efficiencies overtake the falling cross-section. Each muon is required to have $p_T \geq 1.8$ GeV/c, and at least one muon is required to have $p_T \geq 2.8$ GeV/c, due to the first and second trigger level requirements, respectively. The muons are required to have opposite charge and to come from a common vertex. Figure 1 shows the $\mu^+\mu^-$ invariant mass distribution after all the above cuts have been applied. The fitted number of events is 35080 ± 270. The reconstructed J/ψ invariant mass is further required to be within 3σ of its world-average mass, where σ is determined by fitting a Gaussian to the invariant mass distribution.

The transverse momentum distribution of kaons from the $B^+ \rightarrow J/\psi K^+$ decay is considerably harder than for particles from the underlying event. The transverse momentum of a kaon candidate in this channel is required to be greater than 2.0 GeV/c. For the $B^0 \rightarrow J/\psi K^{*0}$, $K^{*0} \rightarrow K^+\pi^-$, decay, any pair of oppositely-charged tracks are considered to be candidates for the K^{*0} decay products. The transverse momentum of the K^{*0} candi-

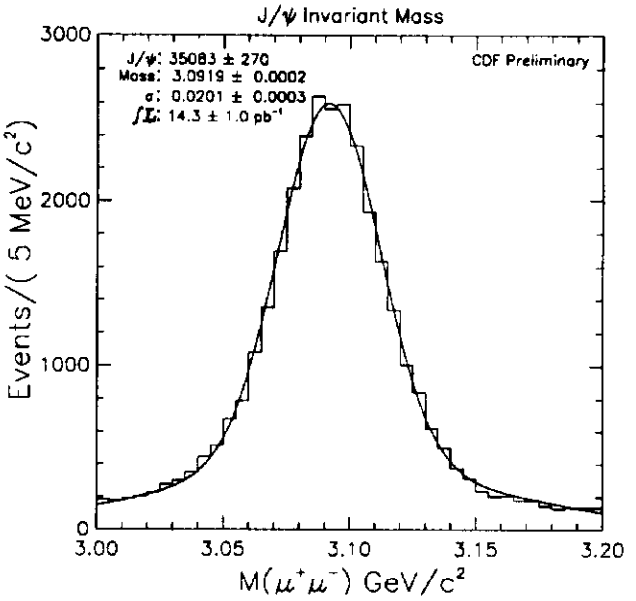

Figure 1: J/ψ invariant mass distribution.

date is required to be greater than 3.5 GeV/c. A cut on the invariant mass of the $K\pi$ pair is also applied. Due to the high background, a K^{*0} mass peak is not observable, but since the detector resolution is much better than the natural width of the K^{*0}, 49.8 MeV/c^2, the requirement 846 MeV/c^2 $\leq m(K\pi) \leq$ 946 MeV/c^2 is imposed. Some fraction of the time, an interchange of the kaon and pion mass assignments can still result in a K^{*0} candidate which passes the cuts. To prevent double-counting, the K^{*0} candidate with the mass closest to the world average K^{*0} mass of 896.1 MeV/c^2 is selected.

Before forming the B meson invariant mass, all the candidate decay product tracks are refit to a common vertex, which improves the momentum resolution, while the dimuon invariant mass is constrained to be equal to the world average J/ψ mass. The B meson transverse momentum is required to be greater than 6.0 GeV/c for the $B^+ \rightarrow J/\psi K^+$ decay, and greater than 9.0 GeV/c for the $B^0 \rightarrow J/\psi K^{*0}$ decay. These cuts determine the minimum p_T for which the total B meson cross-section is measured. Figure 2a shows the reconstructed B invariant mass using the $B^+ \rightarrow J/\psi K^+$ decay channel for $p_T(B) > 6.0$ GeV/c. The peak is fit to a Gaussian plus a linear background(shown as the continuous line) for the range $m(\mu^+\mu^- K) > 5.14$ GeV/c^2, resulting in 104 ± 21 events. The lower mass range (indicated by the dotted line) is excluded from the fit in all the B mass plots since it can include contributions from higher multiplicity B decay modes. The invariant mass distributions for $p_T(B) \geq 9.0$ GeV/c and $p_T(B) \geq 12.0$ GeV/c are shown in Figures 2b and 2c. The fit number of events for these two p_T ranges are 56 ± 12 and 32 ± 8, respectively. Figure 3 shows the invariant mass distribution for B mesons reconstructed in the $B^0 \rightarrow J/\psi K^{*0}$ decay channel, where the fit number of events is 26 ± 8. Since there are sufficient statistics in the $B^+ \rightarrow J/\psi K^+$ decay channel, it has been used to determine the differential B meson cross-section.

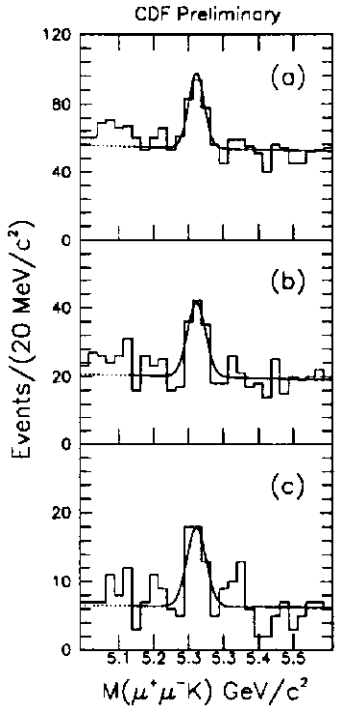

Figure 2: B meson invariant mass from the decay $B^+ \rightarrow J/\psi K^+$ for the following momentum requirements: (a)$p_T(B) \geq 6.0$ GeV/c, (b)$p_T(B) \geq 9.0$ GeV/c, and (c)$p_T(B) \geq 12.0$ GeV/c

The invariant mass distributions for three momentum ranges are shown in Figure 4. The mean and width of the Gaussians are fixed to the values found by fitting the mass distributions used for $p_T(B) \geq 6.0$ GeV/c. The results are 48 ± 14, 24 ± 9, and 13 ± 6 for the momentum ranges 6-9 GeV/c, 9-12 GeV/c, and 12-15 GeV/c, respectively.

The total cross-section is given by

$$\sigma = \frac{N/2}{\mathcal{L} \cdot A \cdot \epsilon \cdot F} \tag{1}$$

where N is the number of events observed, $\mathcal{L}$ is the integrated luminosity, A is the detector acceptance, including the efficiency of the kinematic cuts, ϵ is the combined tracking and track-matching efficiency, and F is the combined branching fraction. The factor of 1/2 is included because decays involving both B and $\overline{B}$ mesons have been reconstructed, but the cross-section is for B mesons only. The differential cross-section, $\frac{d\sigma}{dp_T}$, is similarly given by equation (1) divided by the bin width, Δ_{p_T}, which is equal to 3 GeV/c.

In order to determine the efficiency, a sample of Monte Carlo events was generated, where the b quarks are produced using the next-to-leading order QCD calculation [1, 2], and the MRSD0 [3] structure functions. The b quarks were then fragmented according to the Peterson ansatz [8], using a value of $\epsilon_b = 0.006 \pm 0.001 \pm 0.002$ [9]. The events containing a B^+ meson with $p_T \geq 6.0$ GeV/c or a B^0 meson with $p_T \geq 7.0$ GeV/c were run through a full detector simulation and a parameterization of the first and second trigger level efficiencies.

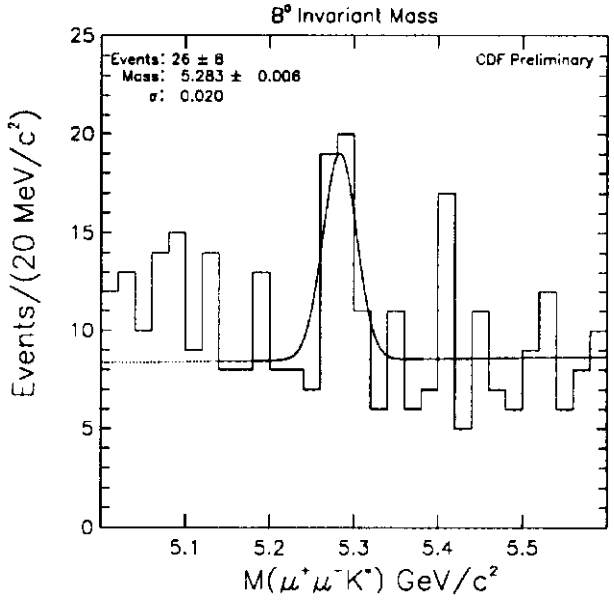

Figure 3: B meson invariant mass from the decay $B^0 \rightarrow J/\psi K^{*0}$.

The combined tracking efficiency for the muon pair has been determined to be 97%, and the tracking efficiency for other decay particles was found to be 92% [5]. The efficiency of the probability requirement of the match between the CTC track and the muon track was measured to be 98.7%. The detector acceptance for each momentum range is given in table 1.

Branching fractions of $(1.12 \pm 0.17) \times 10^{-3}$ and $(1.53 \pm 0.37) \times 10^{-3}$ are used for the $B^+ \rightarrow J/\psi K^+$ and $B^0 \rightarrow J/\psi K^{*0}$ decays, respectively, and a branching fraction of $(5.97 \pm 0.25)\%$ is used for the $J/\psi \rightarrow \mu^+\mu^-$ decay [10]. This gives a combined branching fraction of $(6.7 \pm 1.1) \times 10^{-5}$ for the reconstructed $B^+ \rightarrow J/\psi K^+$decays and $(6.1 \pm 1.6) \times 10^{-5}$ for the reconstructed $B^0 \rightarrow J/\psi K^{*0}$decays, which includes the 2/3 branching fraction for $K^{*0} \rightarrow K^+\pi^-$.

Table 1: Geometric acceptance for the decays $B^+ \rightarrow J/\psi K^+$ and $B^0 \rightarrow J/\psi K^{*0}$.

	$p_T(B)$	Acceptance(%)
B^+	> 6 GeV/c	2.59
	> 9 GeV/c	5.24
	> 12 GeV/c	7.65
	$6 - 9$ GeV/c	0.917
	$9 - 12$ GeV/c	3.36
	$12 - 15$ GeV/c	5.78
B^0	> 7 GeV/c	2.24

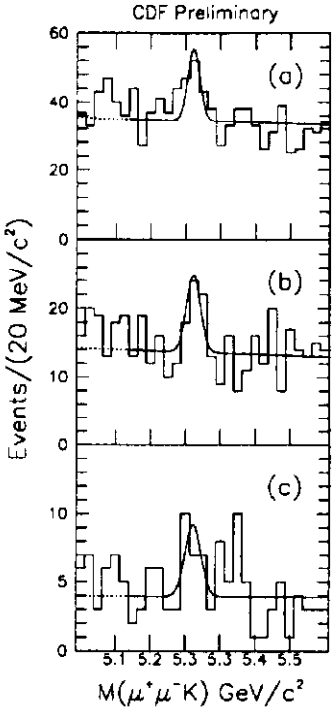

Figure 4: B meson invariant mass from the decay $B^+ \to J/\psi K^+$ for the three momentum ranges, (a) $6.0 < p_T(B) < 9.0$ GeV/c, (b) $9.0 < p_T(B) < 12.0$ GeV/c, and (c) $12.0 < p_T(B) < 15.0$ GeV/c.

A major source of systematic uncertainty in the measurement of the reconstruction efficiency comes from uncertainty in the Monte Carlo model used for event generation and detector simulation. Estimates of the systematic uncertainty are determined by varying the Monte Carlo parameters used to generate the events.

To measure the effect of changing the shape of the assumed production cross-section, the QCD mass scale, μ, is varied between the value $\mu_0 = \sqrt{m_b{}^2 + p_T{}^2}$ and $\mu_0/4$, where m_b, the b quark mass, is taken to be 4.75 GeV/c^2. The QCD parameter, Λ_4, is also varied by 1σ from the central value, as determined from the calculations of the parton distribution functions [3]. The difference in the acceptance between these choices indicates a systematic uncertainty of less than 5%.

The value used for the fragmentation function parameter, ϵ_b, is the result of combining measurements from several different electron-positron experiments [9]. The parameter is varied by $\pm 1\sigma$ from the nominal value, between 0.004 and 0.008. A systematic uncertainty of 7% is associated with this effect.

Recent measurements by CLEO have determined the polarization (Γ_L/Γ) of the decay products from the $B^0 \to J/\psi K^{*0}$ decay to be $(78 \pm 14)\%$ [11]. Varying the polarization within these limits changes the calculated acceptance by $\pm 7\%$.

A study was made of the effect of the trigger efficiency parameterization on the J/ψ acceptance. At the first trigger level, a cut on the slope of the muon chamber track is applied to select tracks with a minimum p_T. Due to multiple scattering, the slope of the

track in the $R-\phi$ plane in the muon chambers can only approximately measure the actual p_T of the muon. Assuming the difference between the p_T estimated by the slope and the true transverse momentum is described by a Gaussian distribution, the trigger efficiency curve is fitted to an error function. It has been determined that variations in the fit values used in the parameterization change the overall acceptance by $\pm 8\%$.

The tracking efficiency of the CTC was determined in the previous run [5]. The measured individual superlayer residuals and hit efficiencies were included in the detector simulation. Simulated tracks were then imbedded in real data samples, and the reconstruction efficiency was determined. This study yielded a systematic uncertainty of $\pm 5\%$. Since one muon and the K^{*0} decay products are allowed to have lower momentum than the particles used in the previous study and to accommodate possible differences in the chamber performance in this run compared to the last one, the systematic uncertainty associated with this efficiency is doubled to $\pm 10\%$.

Another contribution to the systematic uncertainties comes from the method of associating a muon chamber track with a CTC track. Assuming that the algorithm is at least as efficient as it was during the last run, a systematic uncertainty of 8% is assigned, as in reference [5].

A systematic uncertainty of 4% is associated with the reconstruction of kaons which decay in flight inside the CTC volume. This is based on simulation results in which about 8% of the kaons decay in flight and half of these are successfully reconstructed. The 4% uncertainty represents the maximum discrepancy between the ability to reconstruct such tracks in the simulation compared to the data.

Combining these effects in quadrature, the reconstruction efficiency has overall systematic uncertainties of $\pm 19\%$ for the $B^+ \to J/\psi K^+$ decay and $\pm 23\%$ for the $B^0 \to J/\psi K^{*0}$ decay.

There is another possible source of systematic uncertainty that pertains specifically to the differential cross-section measurement. For a finite momentum bin width, merely dividing by the bin width can only approximately convert the cross-section integrated across the bin to a single point on the differential cross-section curve. The proper conversion factor has been estimated from the Monte Carlo simulation. For each p_T bin, the cross-section curve is fitted to an exponential function and the conversion factor is calculated analytically. The measured point is placed at the mean transverse momentum of the bin, which corresponds to 7.2 GeV/c for the first bin, 10.2 GeV/c for the second bin, and 13.2 GeV/c for the third bin. At each of these points, the conversion factor from the Monte Carlo is found to be within 8% of that obtained by dividing by the bin width. Therefore an 8% systematic uncertainty is assigned due to the bin size effect. The conversion factors for each bin are within 2% of one another, so that the shape of the curve defined by the measured differential cross-section points is less sensitive to the binning effect than is the absolute normalization.

The largest single source of systematic uncertainties results from limited knowledge of the branching fractions. This uncertainty is equal to 15% for the $B^+ \to J/\psi K^+$ decay, and 25% for the $B^0 \to J/\psi K^{*0}$ decay [10].

Since the b quark is not directly observable, the Monte Carlo must be used to infer the b quark cross-section from the B meson cross-section. The cross-section is quoted for b quarks with $p_T > p_{T\,min}$, where $p_{T\,min}$ is defined to be a minimum momentum from which at least 90% of the B mesons in the Monte Carlo sample are produced. The b quark $p_{T\,min}$ is determined to be 7.5 GeV/c for $p_T(B) \geq 6.0$ GeV/c, 10.5 GeV/c for $p_T(B) \geq 9.0$ GeV/c,

and 13.5 GeV/c for $p_T(B) \geq 12.0$ GeV/c. Except for this cut applied at the generator level, the determination of the reconstruction efficiency proceeds exactly as for the B meson. For the B production ratios the assumption that 75% of b quarks fragment in equal amounts to the lightest charged and neutral B mesons, with the remaining 25% fragmenting to heavier B mesons and b baryons [12] has been used.

The b quark integrated cross-section measurements are shown in Figure 5.

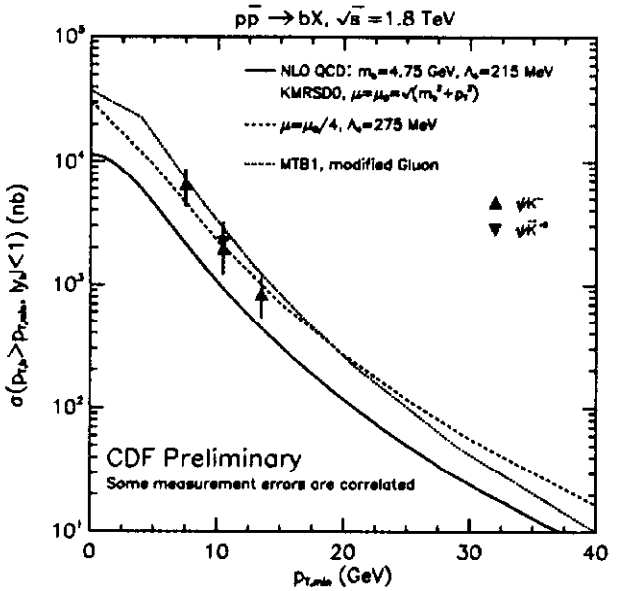

Figure 5: b quark total cross-section. The results of this analysis are shown as diamonds for the $B^+ \rightarrow J/\psi K^+$ decay channel and as an inverted diamond for the $B^0 \rightarrow J/\psi K^{*0}$ decay channel.

For comparison, the next-to-leading order QCD calculated cross-section [13] is shown as the solid line. The theoretical prediction is noticeably lower than the experimental points. The dashed line illustrates how the theoretical cross-section can be changed by varying μ and Λ_4. The dotted line compares a calculation by Berger, Meng and Tung [14] to the data and other theoretical calculations.

The differential cross-section measurements obtained from the $B^+ \rightarrow J/\psi K^+$ decay sample are plotted in Figure 6. A systematic uncertainty of 23%, common to all three points, has been removed from the error bars shown. For comparison, a predicted differential B meson cross-section, corresponding to the solid line on the b quark cross-sections shown in Figure 5, is included. This measurement suggests that the shape of the theoretical cross-section differs from the experimental result as well.

We thank the Fermilab staff and the technical staffs of the participating institutions for their vital contributions. This work was supported by the U.S. Department of Energy and National Science Foundation; the Italian Istituto Nazionale di Fisica Nucleare; the Ministry of Science, Culture, and Education of Japan; the Natural Sciences and Engineering Research Council of Canada; the A. P. Sloan Foundation; and the Alexander von Humboldt-Stiftung.

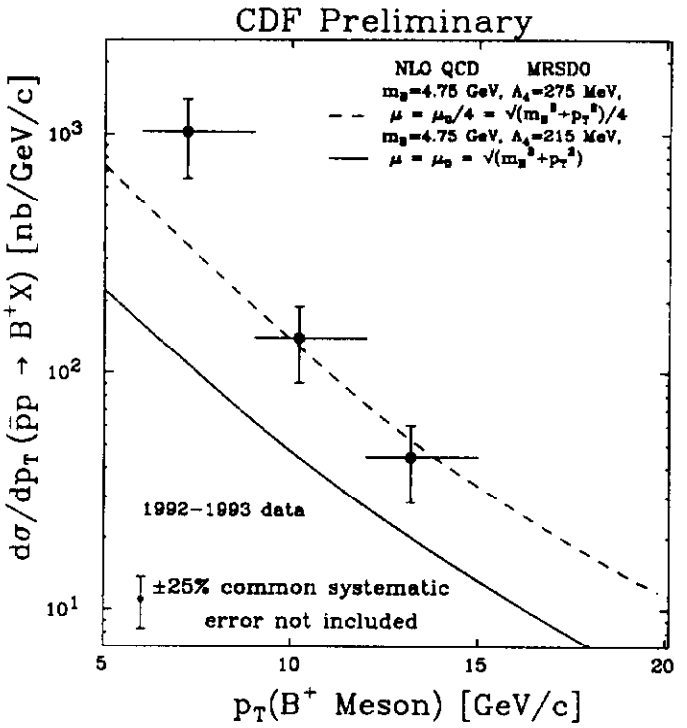

Figure 6: B meson differential cross-section.

1. P. Dawson *et al.*, Nucl. Phys. **B327**, 49 (1988).
2. M. Mangano *et al.*, Nucl. Phys. **B373**, 295 (1992).
3. A. Martin, R. Roberts and J. Stirling, *New Information on the Parton Distributions*, RAL-92-021, DTP/92/16 (1992).
4. F. Abe *et al.*, CDF Collab., Fermilab-Pub-93/158-E (1993), submitted to Phys. Rev. Lett.
5. F. Abe *et al.*, CDF Collab., Phys. Rev. Lett. **68**, 3403 (1992).
6. F. Abe *et al.*, CDF Collab., Submitted to Phys. Rev. D, May 1993.
7. F. Abe *et al.*, CDF Collab., Nucl. Instrum. Methods Phys. Res., Sect. A **271** (1988) 387.
8. C. Peterson *et al.*, Phys. Rev. D **27**, 105 (1983).
9. J. Chrin, Z. Phys. C **36**, 163 (1987).
10. M. S. Alam *et al.* CLEO Collab., contribution 304 to the XVI International Symposium on Lepton and Photon Interactions (1993); the $J\psi$ branching ratio is from M. Aguilar-Benitez *et al.*, Phys. Rev. D **45**, Part 2. (1992).
11. S. Ball, in *The Fermilab Meeting: DPF 92*, Proceedings of the DPF Meeting, Batavia, Illinois, 1992, edited by C. Albright *et al.* (World Scientific, Singapore, 1993), p. 533.
12. B. Adeva *et al.*, L3 Collab., Phys. Lett. B **252**, 703 (1990).
13. M. Mangano, *On the B and J/ψ Cross Section Measurements at UA1 and CDF*, IFUP-TH 2/93, Feb. 1993.
14. E. Berger *et al.* Phys. Rev. D **46**, 1895 (1993).